Generalized oscillator strengths for the valence-shell excitations of argon

Lin-Fan Zhu,[1,*] Hua-Dong Cheng,[1] Zhen-Sheng Yuan,[1] Xiao-Jing Liu,[1] Jian-Min Sun,[1] and Ke-Zun Xu[1]
[1]*Hefei National Laboratory for Physical Sciences at Microscale, Department of Modern Physics, University of Science and Technology of China, Hefei, Anhui, 230026, China*
(Received 12 December 2005; published 7 April 2006)

The generalized oscillator strengths for the valence-shell excitations to $3p^5(4s,4s')$ and $3p^5(4p,4p')$ of argon were measured by an angle-resolved fast-electron energy-loss spectrometer at an incident electron energy of 2500 eV. The transition multipolarities for these excitations were elucidated with the help of the calculated intermediate coupling coefficients using the COWAN code. The generalized oscillator strength profiles for the electric dipole excitations to $3p^5(4s,4s')$, the electric quadrupole and monopole excitations to $3p^5(4p,4p')$ were analyzed and their positions of the extrema were determined. Furthermore, the generalized oscillator strength of the electric quadrupole excitation in $3p \rightarrow 4p$ was determined and its profile is in general agreement with the theoretical calculations. However, the generalized oscillator strength profile of the electric monopole excitation in $3p \rightarrow 4p$ is different from the theoretical calculations.

DOI: 10.1103/PhysRevA.73.042703 PACS number(s): 34.80.Dp, 34.80.Gs, 33.70.Fd, 31.15.Ne

I. INTRODUCTION

The generalized oscillator strength (GOS) can be used to evaluate the theoretical methods, determine the correct spectral assignments [1], and explore the excitation dynamics [2]. The deviation of the magnitudes and positions of the minima or maxima of the GOS predicted by the theoretical calculations from the experimental results will serve as a test of the applicability of the Born approximation as well as the accuracy of the wave functions [3]. From our recent works [4,5], it is known that the GOS ratio is more direct and accurate to rigorously test the theoretical models than the GOS itself, and therein the valence shell transition multipolarities (e.g., electric monopole, electric dipole, and electric quadrupole) of Ne and Kr for fast electron impact have been elucidated with the help of the calculated intermediate coupling coefficients. To the best of our knowledge, the valence shell transition multipolarities of Ar for fast electron impact have not been elucidated in the previous experimental works.

In the previous low energy electron impact studies of Ar, Tam and Brion [6] measured the relative differential cross sections (DCS's) for the excitations to $3p^5(4s,4p)$ configurations at the incident electron energies of 30 and 50 eV. Lewis *et al.* [7] measured the relative DCS's for the excitations to $3p^54s$ configuration at the incident energies of 30, 40, 50, 60, 80, 100, and 120 eV. Chutjian and Cartwright [8] reported the DCS's for the lowest 30 excitations at the incident energies of 16, 20, 30, 50, and 100 eV. Filipović *et al.* [9,10] determined the DCS's for some excitations to $3p^5(4s,4p)$ configurations at five incident energies from 16 to 80 eV. Recently, the DCS's and DCS ratios for the excitations to $3p^54s$ configuration were measured and calculated at the incident energies of 14, 15, 17.5, 20, 30, 50, and 100 eV by Khakoo *et al.* [11].

For the experiments with the intermediate and high energy electron impact, Li *et al.* [12] measured the DCS's and GOS's for the excitations to $3p^5(4s,4s')$ at the incident electron energies of 400 and 500 eV. Bielschowsky *et al.* [13] measured the GOS for the excitations to $3p^5(4s+4s')$ at the incident energy of 1000 eV. Ji *et al.* [14] measured the GOS's of $3p^6 \rightarrow 3p^5(4s,4s',4p+4p')$ at the impact energy of 1500 eV. Fan and Leung [15] determined the GOS's of $3p^6 \rightarrow 3p^5(4s+4s',4p+4p',5s+5s'+3d+3d')$ at the impact energy of 2500 eV. Wong *et al.* [16] observed the minima and maxima in the GOS's for the $3p^6 \rightarrow 3p^5(4s+4s')$ transition of Ar at the incident electron energy of 25 keV.

For the previous theoretical studies at low impact energies, Filipovi ć *et al.* summarized them in their recent works [9,10]. For the excitations to $3p^5(4s+4s')$, Bonham [17] predicted the existence of the maximum and minimum in the GOS within the framework of the first Born approximation (FBA). This work was extended by Shimamura [18]. Bielschowsky *et al.* [13] calculated the GOS's within the framework of the first Born and Glauber approximations. Chen and Msezane [19] calculated the GOS using the methods of Hartree-Fork (HF) and random phase approximation with exchange (RPAE). In addition, Peterson and Allen [20] got a set of semiempirical cross sections for plasma-modeling purposes by combining the Born approximation and the experimental generalized oscillator strengths. Recently, Amusia *et al.* [21] calculated the GOS's for the electric monopole and quadrupole excitations in $3p \rightarrow 4p$ transitions using the methods of HF and RPAE.

With the above survey, it is noticed that most of the works concentrate on the low energy electron impact, in which the transitions between states with different spin multiplicities are possible as a result of the electron exchange effects [22]. However, for the sufficiently fast electron impact, the influence of the incident particle upon an atom or molecule can be regarded as a sudden and small external perturbation. Thus the cross section can be factorized into two factors, one dealing with the incident particle only, the other (GOS) dealing with the target only, and the exchange effect is negligibly small [22]. The GOS was defined as [22–24] (in atomic units)

*Corresponding author. Electronic address: lfzhu@ustc.edu.cn

$$f(E,K)=\frac{E}{2}\frac{p_0}{p_a}K^2\frac{d\sigma}{d\Omega}=\frac{2E}{K^2}\left|\langle\Psi_n|\sum_{j=1}^{N}\exp(i\mathbf{K}\cdot\mathbf{r}_j)|\Psi_0\rangle\right|^2, \tag{1}$$

where E is the excitation energy, K is the momentum transfer, p_0 and p_a are the incident and scattered electron momenta, respectively. $f(E,K)$ and $d\sigma/d\Omega$ stand for GOS and DCS while Ψ_0 and Ψ_n are N electrons wave functions for initial and final states, respectively. $\mathbf{r}_j$ is the position vector of the jth electron.

In the present work, the GOS's for the valence shell excitations to $3p^5(4s,4s')$ and $3p^5(4p,4p')$ of Ar were measured at an incident electron energy of 2500 eV. The transition multipolarities for these excitations were elucidated with the help of our calculated intermediate coupling coefficients using the COWAN code [25]. The GOS profiles for these excitations were analyzed and their positions of the extrema were determined.

II. EXPERIMENTAL AND THEORETICAL METHOD

A. Experimental method

The angle-resolved electron-energy-loss spectrometer (AREELS) used in this experiment has been described in detail in Refs. [26–28]. Briefly, it consists of an electron gun, a hemispherical electrostatic monochromator made of aluminium, a rotatable energy analyzer of the same type, an interaction chamber, a number of cylindrical electrostatic lenses, and a one-dimensional position sensitive detector for detecting the scattered electrons. All of these components are enclosed in four separate vacuum chambers made of stainless steel. The impact energy of the spectrometer can be varied from 1 to 5 keV. For the present measurement the impact energy was set at 2500 eV and the energy resolution was 75 meV [full width at half maximum (FWHM)]. The background pressure in the vacuum chamber was 5×10^{-5} Pa. The scattering angle was calibrated by the angular distribution of the inelastic scattering signal of the excitations to $4s[3/2]_1+4s'[1/2]_1$ around the geometry nominal 0°. The angular resolution was about 0.8° (FWHM) at the present experimental condition.

Similar to our recent work of Ne [5], the method of gas mixture (He and Ar with a fixed proportion) was used in order to reduce the experimental errors and improve the efficiency of the experimental measurement. In the present work, the electron-energy-loss spectra in the energy-loss region of 11–22 eV for Ar+He were measured from 0.5° to 8.5°. A typical electron energy loss spectrum is shown in Fig. 1, where the peaks from A to E are labeled. The peak F corresponds to the excitation to $2\,^1P$ of helium, which is used to calibrate the measured data.

It is known that the corrections of the pressure effect and angular resolution are needed in the method of gas mixture [5]. Because the intensity of double scattering is proportional to the square of the pressure, while the intensity of the single scattering is proportional to the pressure, the relation between the measured intensity ratios and the pressure is expressed as

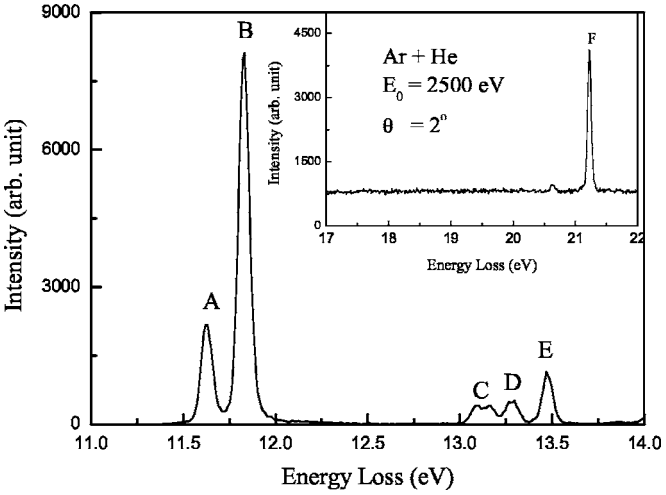

FIG. 1. A typical electron-energy-loss spectrum of Ar+He at the impact energy of 2500 eV and the scattering angle of 2°.

$$\frac{I_p(\theta)}{I_{ref}(\theta)}\approx\left(\frac{I_p(\theta)}{I_{ref}(\theta)}\right)_{P=0}+c(\theta)P, \tag{2}$$

where $c(\theta)$ is a coefficient which depends on the scattering angle and the corresponding elastic and inelastic cross sections of He and Ar [29]. $I_p(\theta)$ and $I_{ref}(\theta)$ represent the intensity of the inelastic excitation of Ar and the intensity of the excitation to $2\,^1P$ of helium, respectively. The values of $[I_p(\theta)/I_{ref}(\theta)]_{P=0}$, which are proportional to the corresponding ratios of cross sections, were obtained by a linear least-squares fitting [30]. Some results of the corrections of the pressure effect are shown in Fig. 2. In addition, the angular resolution has great influence on the measurement of GOS's at small angles. Using the method described in Ref. [31], the influence of angular resolution on the GOS's at small angles was corrected.

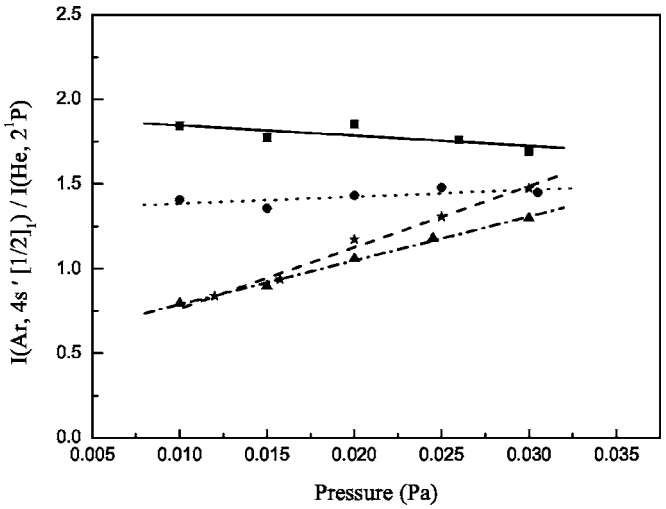

FIG. 2. The pressure effect corrections at the scattering angles of 3.0°(■), 3.5°(●), 4.5°(▲), and 5.0°(★) for the electric dipole excitation to $4s'[1/2]_1$. The lines are the corresponding linearly fitted results.

TABLE I. The intermediate coupling coefficients and the assignments for peaks from *A* to *E*. The energy levels from Moore [37] and from our calculations are listed. *E*0, *E*1, *E*2, *M*1, and *T* represent the electric monopole, electric dipole, electric quadrupole, magnetic dipole, and spin-forbidden transitions from the ground state($3p^6\ ^1S_0$), respectively.

Peak		*JL* designation	Intermediate coupling	Transition	Energy(eV) Cowan	Energy(eV) Moore
		$3p^6$	$0.9973(3p^6\ ^1S_0)$		0.000	0.000
		$3p^54s[3/2]_2$	$0.9981(3p^54s\ ^3P_2)$	T	11.545	11.548
A		$3p^54s[3/2]_1$	$0.8982(3p^54s\ ^3P_1)+0.4355(3p^54s\ ^1P_1)$	$E1$	11.616	11.624
		$3p^54s'[1/2]_0$	$0.9977(3p^54s\ ^3P_0)$	T	11.709	11.723
B		$3p^54s'[1/2]_1$	$-0.4347(3p^54s\ ^3P_1)+0.8993(3p^54s\ ^1P_1)$	$E1$	11.845	11.828
		$3p^54p[1/2]_1$	$-0.1737(3p^54p\ ^3P_1)+0.9756(3p^54p\ ^3S_1)$ $0.1127(3p^54p\ ^1P_1)$	$M1$	12.907	12.907
		$3p^54p[5/2]_3$	$0.9998(3p^54p\ ^3D_3)$	T	13.054	13.076
	C_1	$3p^54p[5/2]_2$	$0.7993(3p^54p\ ^3D_2)-0.1409(3p^54p\ ^3P_2)$	$E2$	13.075	13.095
C			$+0.5839(3p^54p\ ^1D_2)$			
	C_2	$3p^54p[3/2]_2$	$-0.2967(3p^54p\ ^3D_2)+0.7524(3p^54p\ ^3P_2)$ $+0.5878(3p^54p\ ^1D_2)$	$E2$	13.148	13.172
		$3p^54p[3/2]_1$	$0.7252(3p^54p\ ^3D_1)-0.4026(3p^54p\ ^3P_1)$ $-0.5581(3p^54p\ ^1P_1)$	$M1$	13.130	13.153
		$3p^54p'[3/2]_1$	$0.6879(3p^54p\ ^3D_1)+0.4014(3p^54p\ ^3P_1)$ $+0.6042(3p^54p\ ^1P_1)$	$M1$	13.264	13.283
	D_1	$3p^54p[1/2]_0$	$0.9578(3p^54p\ ^3P_0)-0.2800(3p^54p\ ^1S_0)$	E_0	13.255	13.273
D						
	D_2	$3p^54p'[3/2]_2$	$0.5222(3p^54p\ ^3D_2)+0.6430(3p^54p\ ^3P_2)$ $-0.5598(3p^54p\ ^1D_2)$	$E2$	13.270	13.302
		$3p^54p'[1/2]_1$	$0.8037(3p^54p\ ^3P_1)+0.2058(3p^54p\ ^3S_1)$ $-0.5569(3p^54p\ ^1P_1)$	$M1$	13.297	13.328
E		$3p^54p'[1/2]_0$	$0.2862(3p^54p\ ^3P_0)+0.9313(3p^54p\ ^1S_0)$ $-0.1891(3p^55p\ ^1S_0)$	$E0$	13.527	13.480

The relative DCS's for the valence shell excitations of Ar can be determined with the intensity ratio $[I_{Ar}(\theta)/I_{He}(\theta)]_{P=0}$ multiplied by the DCS of the excitation to $2\ ^1P$ of He calculated by Cann and Thakkar [32], which is in excellent agreement with our previous experimental results [33]. Then the relative GOS's were obtained according to Eq. (1). Based on the Lassettre's limit theorem [34], it is known that the GOS converges to the optical oscillator strength (OOS) as $K^2 \rightarrow 0$. The behavior of the GOS near $K^2=0$ is illustrated as

$$f(E_0,K) = \frac{1}{(1+x)^6}\left[f_0 + \sum_{n=1}^{m} f_k\left(\frac{x}{1+x}\right)^n\right], \qquad (3)$$

where f_0 is the OOS and f_k are the fitted constants, $x = K^2/\alpha^2$ with $\alpha=(2I)^{1/2}+[2(I-E)]^{1/2}$, I and E are the ionization and excitation energies, respectively. By fitting the relative GOS of the dipole allowed excitation to $4s'[1/2]_1$ using this Lassettre formula and normalizing the extrapolated result (relative OOS) to the absolute one (0.259) measured by dipole (e,e) method [26], the absolute GOS for the excitation to $4s'[1/2]_1$ can be determined. Then the GOS's for other valence shell excitations can be obtained by making reference to the GOS of the excitation to $4s'[1/2]_1$.

The overall errors in this work come from the statistics of counts δ_s, the angular resolution determination for small angle δ_r, the pressure correction δ_p, and the normalizing procedure δ_n as well as the error resulting from the deconvolution procedure δ_d. In this work, the maximum of each error is $\delta_s=8\%$ for the weakest transition, $\delta_r=5\%$, $\delta_p=5\%$, $\delta_n=5\%$, and $\delta_d=10\%$. The total errors are less than 15%.

B. Calculational method

The calculations of the intermediate coupling coefficients for the lowest 14 levels of Ar were performed with the COWAN code [25]. The method of calculation was described in detail by Clark *et al.* [35,36], and summarized briefly in our recent work [5]. The one-electron radial wave functions for each of the electron configurations with the Hartree-Fock method were first calculated so as to minimize the center-of-gravity energy of the configuration. Then the configuration interaction was included when calculating the Coulomb integrations between each pair of the configurations. The energy matrices were set up for each possible value of the total angular momentum J, and the eigenstates and eigenvalues are then obtained through diagonalizing each matrices on the given basis set.

For the present calculations a 21 configuration basis set was used, and the calculated excitation energies are consistent with the Moore levels [37] within 0.07 eV. The calcu-

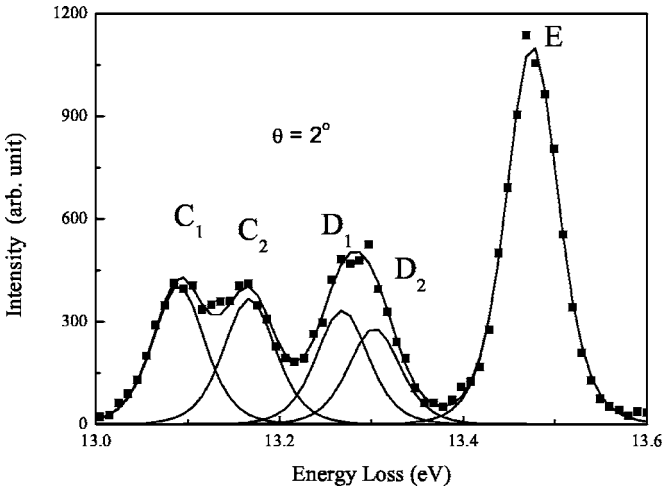

FIG. 3. The deconvolved results of the spectrum for the peaks *C*, *D*, and *E* shown in Fig. 1. ■, the experimental data; –, the deconvolved results.

lated intermediate coupling coefficients and the energy levels are listed in Table I.

III. RESULTS AND DISCUSSIONS

From Table I we notice that there exit singlet and triplet *LS* components in the intermediate coupling scheme. Since the probability for the spin-forbidden transition in connection with the electron-exchange effect is negligibly small for fast electron impact [22], the contributions of the excitations from the ground state $^1S_0$ to the triplet components can be neglected. Thus the excited states, e.g., $4s[3/2]_2$, $4s'[1/2]_0$, and $4p[5/2]_3$, which only consist of the triplet components in the intermediate coupling scheme (see Table I), were not observed in the present spectra. In addition, the excitations to $4p[1/2]_1$, $4p[3/2]_1$, $4p'[3/2]_1$, and $4p'[1/2]_1$, which correspond to the magnetic dipole excitations based on the singlet components in the intermediate coupling scheme, should not appear in the present spectra [4,5,38]. Therefore, the observed transitions of Ar in our concerned energy region consist of the ones to $3p^5(4p,5p)\ ^1S_0$, $3p^54s\ ^1P_1$, and $3p^54p\ ^1D_2$, which correspond to the electric monopole, electric dipole, and electric quadrupole excitations, respectively. Based upon above discussion, the transition multipolarities for *A* to *E* were assigned, as shown in Table I. It is noticed that the peak *C* and *D* include two excitations, respectively. Figure 3 shows the deconvolved result of the spectrum at the scattering angle of 2° for the peak *C*, *D*, and *E*.

In the following we will discuss the GOS's for the valence shell excitations of Ar (the data are shown in Table II). First, the experimental GOS's of the electric dipole transitions to $4s[3/2]_1$ and $4s'[1/2]_1$ are shown in Fig. 4. It can be seen that the GOS's measured by Ji *et al.* [14] at the incident electron energy of 1500 eV are generally consistent with the present results except for some points. The deviation may be due to the large experimental errors in the work of Ji *et al.*, therein the single channel detector of channeltron was used. The experimental results measured by Li *et al.* [12] at the incident electron energies of 400 and 500 eV are in agreement with ours in the region of $K^2 < 0.35$ a.u., but they are generally lower than the present ones in the large K^2 region. This difference may be attributed to the fact that the first Born approximation (FBA) is not reached in the large K^2 region.

In order to compare with the previous experimental and theoretical works, the sum of the GOS's for the excitations to $4s[3/2]_1$ and $4s'[1/2]_1$ are shown in Figs. 5 and 6, respec-

TABLE II. The GOS's for the resolved excitations to $3p^5(4s,4s',4p,4p')$ of Ar. The number in square brackets denote the power of ten.

K^2(a.u.)	$4s[3/2]_1$	$4s'[1/2]_1$	$4p[5/2]_2$	$4p[3/2]_2$	$4p'[3/2]_2$	$4p[1/2]_0$	$4p'[1/2]_0$
0.019	7.67[−2]	2.52[−1]					
0.061	5.02[−2]	1.82[−1]	2.32[−3]	1.65[−3]	1.73[−3]	1.12[−3]	5.50[−3]
0.13	4.00[−2]	1.41[−1]	3.59[−3]	3.04[−3]	2.40[−3]	2.56[−3]	9.67[−3]
0.23	2.83[−2]	1.11[−1]	5.59[−3]	5.02[−3]	4.05[−3]	3.73[−3]	1.47[−2]
0.35	1.93[−2]	7.48[−2]	5.52[−3]	5.04[−3]	4.09[−3]	4.55[−3]	1.65[−2]
0.51	1.25[−2]	4.82[−2]	5.19[−3]	4.48[−3]	2.92[−3]	5.01[−3]	1.55[−2]
0.69	6.58[−3]	2.63[−2]	3.51[−3]	3.45[−3]	2.43[−3]	3.93[−3]	1.29[−2]
0.90	3.49[−3]	1.29[−2]	2.32[−3]	2.00[−3]	2.04[−3]	2.33[−3]	9.33[−3]
1.14	1.60[−3]	5.81[−3]	1.06[−3]	1.23[−3]	1.04[−3]	1.94[−3]	6.32[−3]
1.40	8.36[−4]	3.20[−3]	6.97[−4]	7.32[−4]	5.02[−4]	1.27[−3]	4.70[−3]
1.69	1.09[−3]	4.03[−3]	2.63[−4]	3.28[−4]	3.84[−4]	4.15[−4]	2.86[−3]
2.01	1.12[−3]	4.82[−3]	1.83[−4]	1.21[−4]	8.47[−5]	3.97[−4]	1.79[−3]
2.36	9.49[−4]	4.29[−3]	1.59[−4]	1.03[−4]	6.20[−5]	3.93[−4]	1.52[−3]
2.74	1.29[−3]	4.85[−3]	2.06[−4]	2.41[−4]	2.17[−4]	4.18[−4]	1.58[−3]
3.14	1.00[−3]	4.24[−3]	2.56[−4]	2.12[−4]	1.38[−4]	4.98[−4]	1.53[−3]
3.57	8.23[−4]	3.11[−3]	2.69[−4]	2.01[−4]	1.62[−4]	3.24[−4]	1.30[−3]
4.03	7.09[−4]	2.73[−3]	2.33[−4]	1.86[−4]	2.08[−4]	2.73[−4]	1.03[−3]

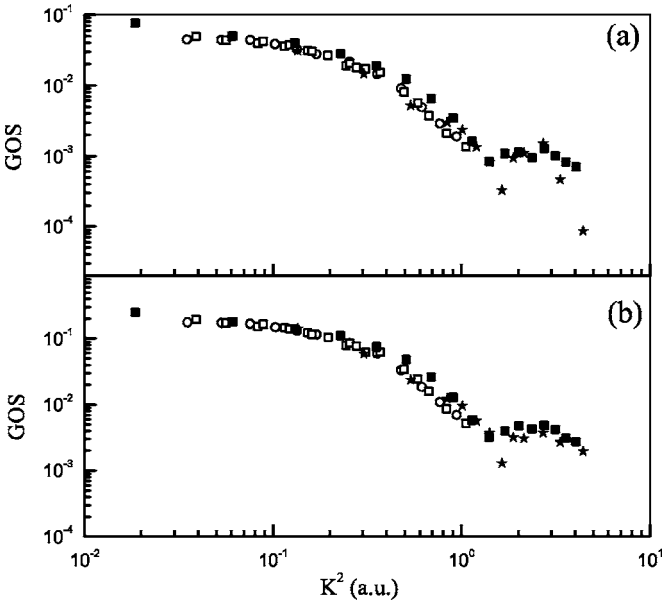

FIG. 4. The GOS's for the excitations to (a) $4s[3/2]_1$ and (b) $4s'[1/2]_1$. ■, present results; ○, Li *et al.* [12] at 400 eV; □, Li *et al.* [12] at 500 eV; ★, Ji *et al.* [14] at 1500 eV.

tively. From Fig. 5 it can be seen that the results measured by Fan and Leung [15] at the incident energy of 2500 eV are in good agreement with the present results, but the results measured by Wong *et al.* [16] at the incident energy of 25 keV and by Bielschowsky *et al.* [13] at the incident energy of 1000 eV are greatly larger than the present results in the large K^2 region. It is noticed that the relative GOS of Wong *et al.* [16] was normalized to the present data at $K^2=0.507$ a.u. This difference may be attributed to the fact that the pressure effect was not corrected in their works. Figure 6(a) compares the present result with other theoretical calculations [13,17–19]. It is noticed that the calculated results by

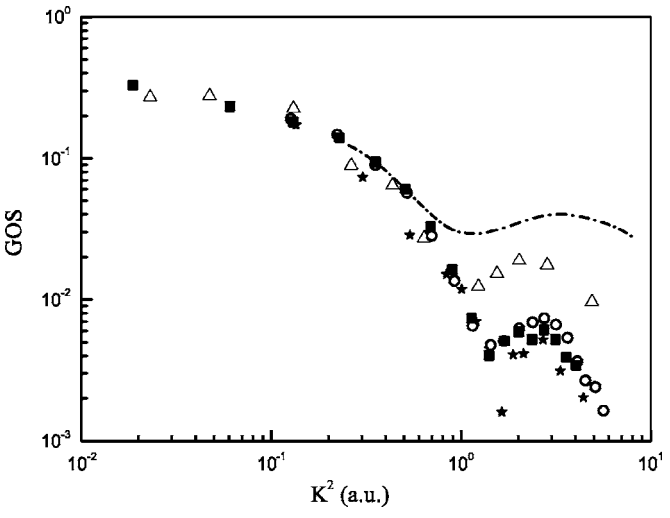

FIG. 5. The GOS for the excitations to $4s[3/2]_1+4s'[1/2]_1$ and the comparison with previous experimental results. ■, present results; △, Bielschowsky *et al.* [13] at 1000 eV; ★, Ji *et al.* [14] at 1500 eV; ○, Fan and Leung [15] at 2500 eV; –·–·, Wong *et al.* [16] at 25 keV.

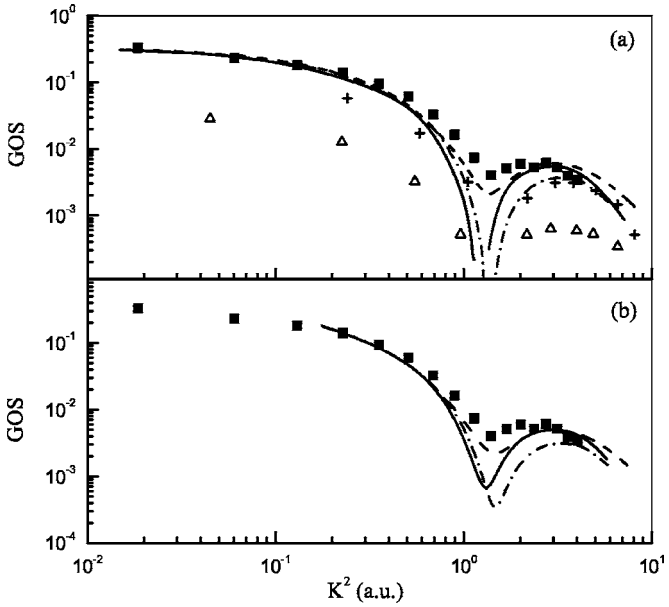

FIG. 6. (a) Same as Fig. 5, but compared with the available theoretical calculations. (b) The influence of the angular resolution is considered for the theoretical results. ■, present results; –, FBA [13]; – –, Glauber YFC [13]; △, FBA [17]; +, FBA, [18]; –·–·, RPAE [19].

Bonham [17] and Shimamura [18] within the framework of the FBA only predicts the GOS profile. The GOS values calculated by Bielschowsky *et al.* [13] within the frameworks of the FBA and Glauber approximation (Yukawa frozen core) and by Chen and Msezane [19] using the method of RPAE are well consistent with the present ones except in the K^2 region near minimum, even when the influence of the angular resolution is considered (see Fig. 6(b), wherein the theoretical GOS's were convolved with the present angular response Gauss function $A(u)$ [5,30]).

The positions of the extrema of the GOS's for the excitations to $4s[3/2]_1$, $4s'[1/2]_1$, and $4s[3/2]_1+4s'[1/2]_1$ are listed in Table III. Because these transitions have the same singlet component in the intermediate scheme (see Table I), the present positions of extreme are in good agreement with each other. It can also be seen that the present positions of the minimum are in agreement with the experimental ones [14,15] and the theoretical results [13,19]. Because the GOS of Wong *et al.* [16] is larger than ours at the large K^2, this results the shift of the minimum position to smaller K^2. It also can be seen that the present positions of the maximum are in agreement with the experimental one by Ji *et al.* [14], but all other experimental and theoretical results [13,15,16,19] are larger than the present ones.

Second, we will discuss the dipole-forbidden transitions of $3p^6 \rightarrow 3p^5(4p,4p')$. In the present work the GOS's for the five transitions (see Fig. 3) were determined respectively (the data are shown in Table II). Although Ji *et al.* [14] and Fan and Leung [15] measured the GOS at the incident energies of 1500 and 2500 eV respectively, the GOS's for the excitations included in $3p^6 \rightarrow 3p^5(4p,4p')$ are not resolved in their works because of their limited energy resolution. Figure 7 shows the GOS for the excitations to $3p^5(4p+4p')$. Although

TABLE III. The positions of the minimum and maximum for the GOS of $3p^6 \rightarrow 3p^5(4s,4s',4s+4s')$ in Ar.

	Experimental						Theoretical		
	$4s[3/2]_1$	$4s'[1/2]_1$	$4s[3/2]_1+4s'[1/2]_1$						
K^2 (a.u.)			Present	Ref. [14]	Ref. [15]	Ref. [16]	Ref. [19]	Ref. [13][a]	Ref. [19][a]
Minimum	1.44±0.1	1.42±0.1	1.43±0.1	1.6	1.35	1.25	1.33	1.48	1.48
Maximum	2.41±0.2	2.34±0.2	2.35±0.2	2.6	2.79	2.96	3.06	3.02	3.29

[a]The influence of the present angular resolution is considered. The results of Ref. [13] refer to the calculation of Glauber approximation.

there are large differences in absolute values among different works, the positions of the maximum are in good consistency except for that of Fan and Leung [15]. The lower values in the K^2 region of 0.3–1.7 a.u. measured by Ji *et al.* [14] may be due to that FBA is not reached at the incident electron energy of 1500 eV. The much larger values measured by Fan and Leung [15] may be attributed to the pressure effect and their deconvolution error.

The GOS's for the electric quadrupole excitations to $4p[5/2]_2$, $4p[3/2]_2$, and $4p'[3/2]_2$ are shown in Figs. 8(a)–8(c), respectively. Because these three transitions have the same singlet component in the intermediate scheme (see Table I), their GOS profiles have similar profile, i.e., two maxima and one minimum. This type of profile was also predicted for the GOS's of the electric quadrupole transitions in Ne and Kr by the theoretical calculations [21], and it has been observed in Kr [4,30]. Based on the calculated intermediate coupling coefficients (see Table I), it is known that the sum of the GOS's for the excitations to $4p[5/2]_2$, $4p[3/2]_2$, and $4p'[3/2]_2$ correspond to the one of the electric quadrupole excitation in Ar $3p \rightarrow 4p$. Figure 9 shows the present result and compared with the calculated ones by Amusia *et al.* [21] using the methods of HF and RPAE. It is noticed that the present GOS profile is in general consistency with the theoretical results by Amusia *et al.* [21], however, there exists difference between them for the absolute values.

The positions of the extrema of the GOS's for the electric quadrupole excitations to $4p[5/2]_2$, $4p[3/2]_2$, $4p'[3/2]_2$, and $4p[5/2]_2+4p[3/2]_2+4p'[3/2]_2$ are listed in Table IV. It can be seen that the present positions of extrema are in good agreement with each other, this is understood since these

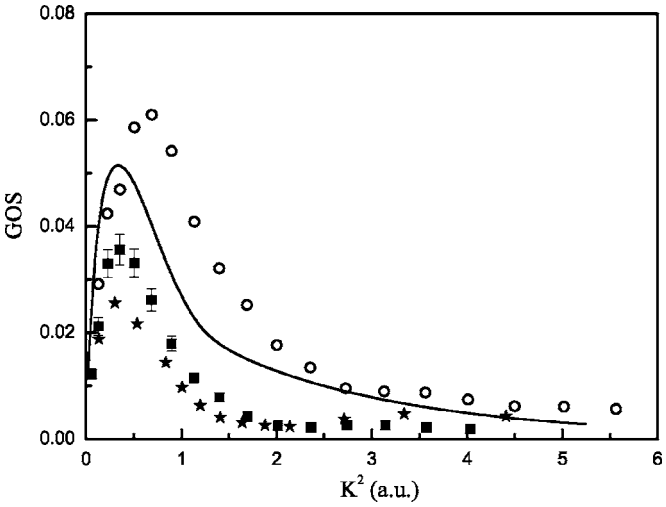

FIG. 7. The GOS for the excitations to $3p^5(4p+4p')$. ■, present results; ★, Ji *et al.* [14] at 1500 eV; ○, Fan and Leung [15] at 2500 eV; –, RPAE calculation [21].

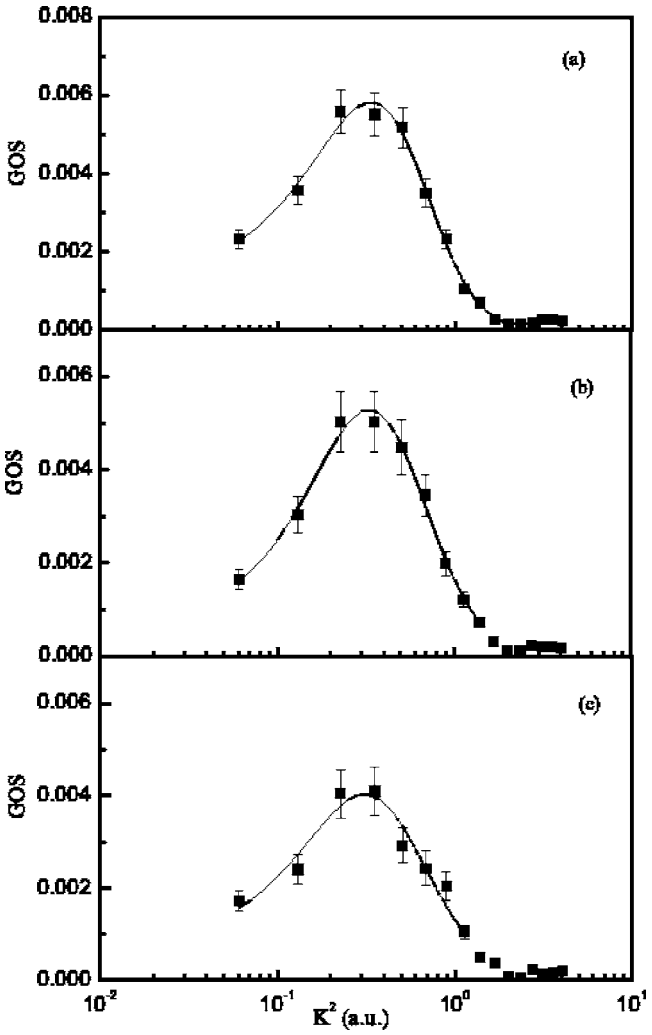

FIG. 8. The GOS's for the electric quadrupole excitations to (a) $4p[5/2]_2$, (b) $4p[3/2]_2$, and (c) $4p'[3/2]_2$. ■, present experimental results; –, present fitted results.

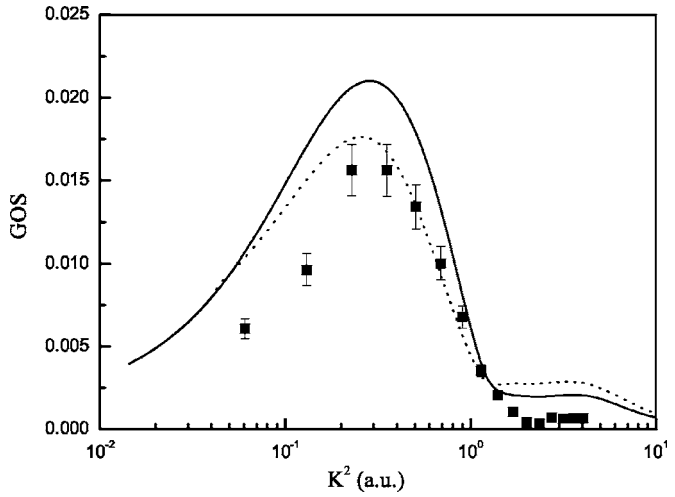

FIG. 9. The GOS for the electric quadrupole excitations in Ar $3p \rightarrow 4p$. ■, present results; –, RPAE calculation [21]; ···, HF calculation [21].

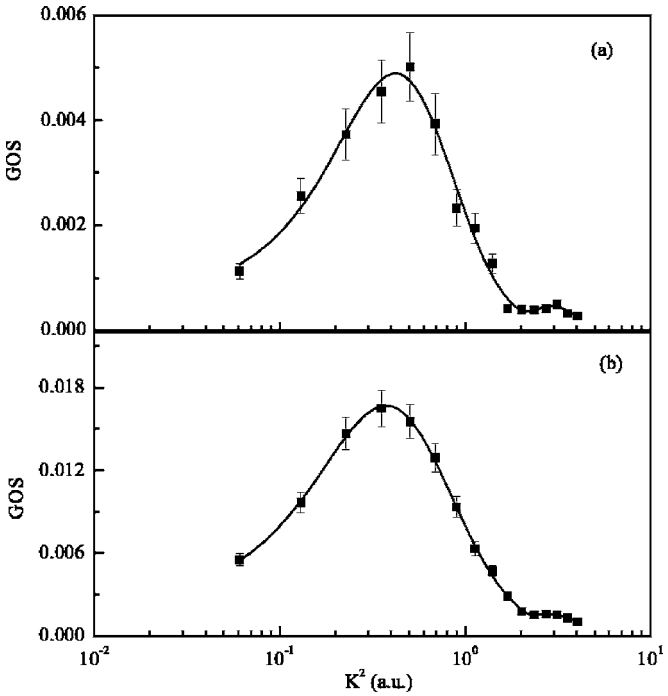

FIG. 10. The GOS's for the electric monopole excitations to (a) $4p[1/2]_0$ and (b) $4p'[1/2]_0$. ■, present experimental results; –, present fitted results.

transitions have the same singlet component in the intermediate scheme (see Table I). Because the GOS's in the larger K^2 region for $4p'[3/2]_2$ and $4p[5/2]_2+4p[3/2]_2+4p'[3/2]_2$ are shoulder, their second maxima are absent in Table IV. Furthermore, the theoretically calculated extrema are in agreement with the expermental results [21].

The GOS's for the electric monopole excitations to $4p[1/2]_0$ and $4p'[1/2]_0$ are shown in Figs. 10(a) and 10(b), respectively. The sum of GOS's for the two excitations, which corresponds to the one for the electric monopole excitations in Ar $3p \rightarrow 4p$, is shown in Fig. 11. It can be seen that the GOS profiles have two maxima and one minimum, similar GOS profiles have been observed for the electric monopole transitions in Kr [4,30]. These experimental observations are different from the theoretical predictions by Amusia *et al.* [21], therein only one maximum exists. However, the second maximum for the electric monopole transition in Ne is absent [5], this is in agreement with the theoretical predictions by Amusia *et al.* [21]. It should be noticed that the measured GOS's for the electric monopole excitation at lower incident electron energies of 300, 400, and 500 eV of Ne have two maxima [39], which is similar to the measured GOS's for the electric monopole excitations at 2500 eV of Ar and Kr [4,30]. This phenomena may be explained that the FBA is not reached for the electric monopole excitations at 2500 eV for Ar and Kr. So further experimental and theoretical investigations are recommended.

The positions of the extrema of the GOS's for the electric monopole excitations to $4p[1/2]_0$, $4p'[1/2]_0$, and $4p[1/2]_0+4p'[1/2]_0$ are listed in Table IV. Similar to the electric quadrupole excitations, the present positions of extrema are in good agreement with each other because these transitions have the same singlet component in the intermediate scheme (see Table I). As discussed above, the theoretical calculation has only one maximum [21], it is slightly larger than the present first maximum.

TABLE IV. The positions of the minimum and maximum for GOS's of $3p^6 \rightarrow 3p^5(4p, 4p', 4p+4p')$ transitions of Ar.

	Present			Theoretical [21]		
		Maximum			Maximum	
K^2 (a.u.)	Minimum	First	Second	Minimum	First	Second
$4p[5/2]_2$	2.29±0.1	0.33±0.05	3.43±0.2			
$4p[3/2]_2$	2.28±0.1	0.33±0.05	3.34±0.2			
$4p'[3/2]_2$	2.41±0.1	0.31±0.05				
$4p[5/2]_2+4p[3/2]_2+4p'[3/2]_2$	2.22±0.1	0.29±0.05		1.99	0.25	3.61
$4p[1/2]_0$	2.17±0.1	0.42±0.05	2.91±0.2			
$4p'[1/2]_0$	2.38±0.1	0.37±0.05	2.83±0.2			
$4p[1/2]_0+4p'[1/2]_0$	2.35±0.1	0.41±0.05	2.94±0.2		0.5	

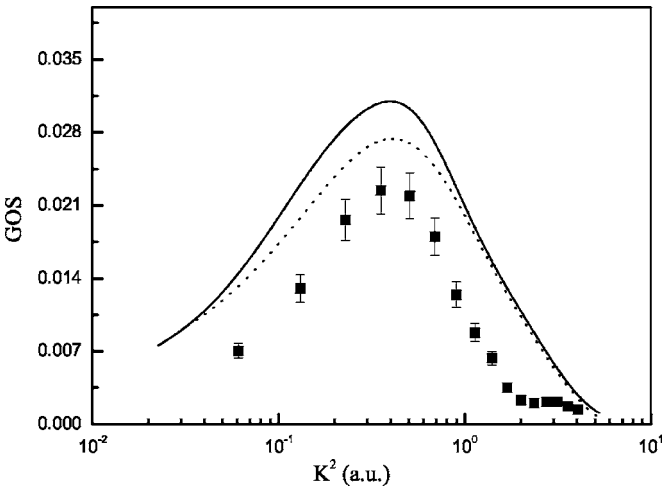

FIG. 11. The GOS for the electric monopole excitations in Ar $3p \rightarrow 4p$. ■, present results; –, RPAE calculation [21]; ···, HF calculation [21].

IV. SUMMARY AND CONCLUSION

The GOS's for the excitations to $3p^5(4s,4s',4p,4p')$ of Ar have been determined with better energy resolution at the incident electron energy of 2500 eV using the method of mixed gas of helium and argon. The excitations are classified as the electric monopole, electric dipole, and electric quadrupole transitions with the help of our calculated intermediate coupling coefficients.

The present minimum positions for the GOS's of the electric dipole excitations to $4s[3/2]_1$, $4s'[1/2]_1$, and $4s[3/2]_1 + 4s'[1/2]_1$ are in agreement with other experimental results [14–16] and theoretical calculations [13,19]. However, for the maximum there is an obvious difference between the present results and other experimental and theoretical ones except for being in agreement with the result measured by Ji *et al.* [14]. The GOS's for the electric quadrupole excitations to $4p[5/2]_2$, $4p[3/2]_2$, and $4p'[3/2]_2$, as well as the electric monopole excitations to $4p[1/2]_0$ and $4p'[1/2]_0$, were reported. Furthermore, the GOS profiles and the extrema positions of the electric quadrupole excitations are in general agreement with the theoretical calculations by Amusia *et al.* [21]. However, for the electric monopole excitations, the theoretical GOS profile [21] has one maximum in the present K^2 region, which is different from the present ones (two maxima). So further experimental and theoretical investigations for the electric monopole and electric quadrupole excitations are recommended.

ACKNOWLEDGMENTS

This work was supported by the National Nature Science Foundation of China (Grants No. 10474089 and No. 10134010) are gratefully acknowledged.

[1] C. C. Turci, J. T. Francis, T. Tyliszczak, G. G. de Souza, and A. P. Hitchcock, Phys. Rev. A **52**, 4678 (1995).
[2] X. J. Liu, L. F. Zhu, Z. S. Yuan, W. B. Li, H. D. Cheng, Y. P. Huang, Z. P. Zhong, K. Z. Xu, and J. M. Li, Phys. Rev. Lett. **91**, 193203 (2003).
[3] Y. K. Kim, M. Inokuti, G. E. Chamberlain, and S. R. Mielczarek, Phys. Rev. Lett. **21**, 1146 (1968).
[4] H. D. Cheng, L. F. Zhu, X. J. Liu, Z. S. Yuan, W. B. Li, and K. Z. Xu, Phys. Rev. A **71**, 032714 (2005).
[5] H. D. Cheng, L. F. Zhu, Z. S. Yuan, X. J. Liu, J. M. Sun, W. C. Jiang, and K. Z. Xu, Phys. Rev. A **72**, 012715 (2005).
[6] W. C. Tam and C. E. Brion, J. Electron Spectrosc. Relat. Phenom. **2**, 111 (1973).
[7] B. R. Lewis, E. Weigold, and P. J. O. Teubner, J. Phys. B **8**, 212 (1975).
[8] A. Chutjian and D. C. Cartwright, Phys. Rev. A **23**, 2178 (1981).
[9] D. M. Filipović, B. P. Marinković, V. Pejčev, and L. Vušković, J. Phys. B **33**, 677 (2000).
[10] D. M. Filipović, B. P. Marinković, V. Pejčev, and L. Vušković, J. Phys. B **33**, 2081 (2000).
[11] M. A. Khakoo, P. Vandeventer, J. G. Childers, I. Kanik, C. J. Fontes, K. Bartschat, K. Bartschat, V. Zeman, D. H. Madison, S. Saxena, R. Srivastava, and A. D. Stauffer, J. Phys. B **37**, 247 (2004).
[12] G. P. Li, T. Takayanagi, K. Wakiya, H. Suanki, T. Ajiro, S. Yagi, S. S. Kano, and H. Takuma, Phys. Rev. A **38**, 1240 (1988).
[13] C. E. Bielschowsky, G. G. B. de Souza, C. A. Lusas, and H. M. Boechat Roberty, Phys. Rev. A **38**, 3405 (1988).
[14] Q. Ji, S. L. Wu, R. F. Feng, X. J. Zhang, L. F. Zhu, Z. P. Zhong, K. Z. Xu, and Y. Zheng, Phys. Rev. A **54**, 2786 (1996).
[15] X. W. Fan and K. T. Leung, Phys. Rev. A **62**, 062703 (2000).
[16] T. C. Wong, J. S. Lee, and R. A. Bonham, Phys. Rev. A **11**, 1963 (1975).
[17] R. A. Bonham, J. Chem. Phys. **36**, 3260 (1962).
[18] I. Shimamura, J. Phys. Soc. Jpn. **30**, 824 (1971).
[19] Z. Chen, A. Z. Msezane, and M. Y. Amusia, Phys. Rev. A **60**, 5115 (1999).
[20] L. R. Peterson and J. E. Allen, Jr., J. Chem. Phys. **56**, 6068 (1972).
[21] M. Y. Amusia, L. V. Chernysheva, Z. Felfli, and A. Z. Msezane, Phys. Rev. A **67**, 022703 (2003).
[22] M. Inokuti, Rev. Mod. Phys. **43**, 297 (1971).
[23] H. Bethe, Ann. Phys. **5**, 325 (1930); Z. Phys. **76**, 293 (1930).
[24] B. G. Tian and J. M. Li, Acta Phys. Sin. **33**, 1401 (1984).
[25] J. J. Abdallah, R. E. H. Clark, and R. D. Cowan, *Los Alamos National Laboratory Manual*, No. LA-11436-M, 1988, Vol. I (unpublished).
[26] S. L. Wu, Z. P. Zhong, R. F. Feng, S. L. Xing, B. X. Yang, and K. Z. Xu, Phys. Rev. A **51**, 4494 (1995).
[27] K. Z. Xu, R. F. Feng, S. L. Wu, Q. Ji, X. J. Zhang, Z. P. Zhong, and Y. Zheng, Phys. Rev. A **53**, 3081 (1996).
[28] X. J. Liu, L. F. Zhu, X. M. Jiang, Z. S. Yuan, B. Cai, X. J. Chen, and K. Z. Xu, Rev. Sci. Instrum. **72**, 3357 (2001).
[29] L. F. Zhu, X. J. Liu, W. B. Li, Z. S. Yuan, H. D. Cheng, Z. P.

Zhong, and K. Z. Xu, Nucl. Phys. Rev. **19**, 150 (2002) (In Chinese).
[30] W. B. Li, L. F. Zhu, X. J. Liu, Z. S. Yuan, J. M. Sun, H. D. Cheng, Z. P. Zhong, and K. Z. Xu, Phys. Rev. A **67**, 062708 (2003).
[31] L. F. Zhu, Z. P. Zhong, X. J. Liu, R. F. Feng, X. J. Zhang, and K. Z. Xu, J. Phys. B **32**, 4897 (1999).
[32] N. M. Cann and A. J. Thakkar, J. Electron Spectrosc. Relat. Phenom. **123**, 143 (2002).
[33] X. J. Liu, L. F. Zhu, Z. S. Yuan, W. B. Li, H. D. Cheng, J. M. Sun, and K. Z. Xu, J. Electron Spectrosc. Relat. Phenom. **135**, 15 (2004).
[34] E. N. Lassettre, J. Chem. Phys. **43**, 4479 (1965); K. N. Klump and E. N. Lassettre, *ibid.* **68**, 886 (1978).
[35] R. E. H. Clark, J. Abdallah, Jr., G. Csanak, and S. P. Kramer, Phys. Rev. A **40**, 2935 (1989).
[36] R. E. H. Clark, G. Csanak, and J. Abdallah, Jr., Phys. Rev. A **44**, 2874 (1991).
[37] C. E. Moore, *Atomic Energy Levels*, Vol. 2 (U. S. GPO, Washington, D. C., 1971).
[38] R. D. Cowan, *The Theory of Atomic Structure and Spectra* (University of California Press, Berkeley, California, 1981).
[39] T. Y. Suzuki, H. Suzuki, S. Ohtani, B. S. Min, T. Takayanagi, and K. Wakiya, Phys. Rev. A **49**, 4578 (1994).